Design Optimised Metasurface Dual Band Antenna and Analysis for 5G Mobile Broadband Use

Mr. V. Appala Raju, V. Navyasree, S. Sri Likith, S. Sandeep, Srinivas Chowdary

Electronics and Communication Engineering Department, VIIT, Visakhapatnam, India,
E-mail: appalarajuvadaboyina2@gmail.com ,vnsri2003@gmail.com

Abstract—
For 5G mobile broadband applications, this research offers a ground-breaking method that blends the metasurface with a unique structural antenna [1]. Utilising a T-shaped slot combination with a square microstrip patch, the host antenna was created on a FR-4 epoxy substrate. A 4×4 square array metasurface has been built on a different identically sized Rogers RT/Duroid 5880(tm) substrate, serving as a superstrate layer and being separated from the original patch by a layer of metasurface [1]. The suggested antenna has an impedance bandwidth of 10 dB between 5.17 GHz and 5.44 GHz. The suggested antenna's axial ratio (AR) bandwidth is in the range of 6.02 GHz to 6.35 GHz. The antenna was used to attain a maximum realised gain of 8.3 dB in the 5.17 GHz to 6.35 GHz range, and it was discovered that the antenna is naturally linearly polarized [3]. Applications for the planned LP antenna include weather radar systems, satellite communication, 5G mobile applications, and more.

Index Terms: Metasurface, Rogers RT/Duroid, Broadband applications, radiation efficiency.

I INTRODUCTION

Flexible antennas have shown considerable growth as they are light weight, The constant advancement of wireless communication technology has been fueled by the widespread need for fast internet access, minimal latency, and seamless connectivity [2]. The need for effective and flexible antenna systems to support these developments is more important than ever as we approach the fifth-generation (5G) revolution. For the introduction of 5G mobile broadband, the 3-6 GHz frequency band in particular is crucial since it balances the trade-offs between capacity, data rates, and coverage [1].

In order to particularly meet the needs of 5G mobile broadband applications, this paper presents a thorough investigation into the design and analysis of a high-performance metasurface antenna that has been developed to function within the 3-6 GHz frequency band [5]. Because they provide unmatched control over electromagnetic wave propagation, Metasurfaces—which are made of subwavelength structured materials—are a great option for designing small, effective, and adaptable antenna systems that can meet the needs of next-generation communication protocols.

The main objective of this research is to combine state-of-the-art electromagnetic theory, computational modelling techniques, and innovative engineering methodologies to create a metasurface antenna that can meet the demanding specifications of 5G mobile broadband communication within the designated frequency range. By carefully modifying the geometric parameters and material properties of the metasurface structure, our design seeks to optimise radiation efficiency, bandwidth, polarisation purity, and beam-steering capabilities, providing robust and trustworthy performance in real-world deployment scenarios [2].

I. METASURFCE SUPERSTRATE PATCH DESIGN

One of the most recent developments in antenna theory is the use of microstrip antennas. Its many benefits include low profile, lightweight, and compact construction, as well as ease of production and integration into arrays [9]. The dimensions of an antenna have a close correlation with its performance parameters [10–12]. The suggested rectangle patch with additional slots is displayed in Figure a. The material that is suggested for the antenna substrate is FR-4. The substrate is 70 x 60 mm in length and breadth, with a height of 1.6 mm. The substrate's top layer is metalized with a rectangular patch of 11.7 x 33.5 mm in length and breadth. Etched on the patch are a T-shaped rectangular slot measuring 30 mm in length and 0.5 mm in width, as well as a cross rectangular slot measuring 15 mm in length and 2 mm in width. A 50Ω input impedance inset feed line measuring 18.1 mm in length and 3 mm in width is introduced into the radiating patch.

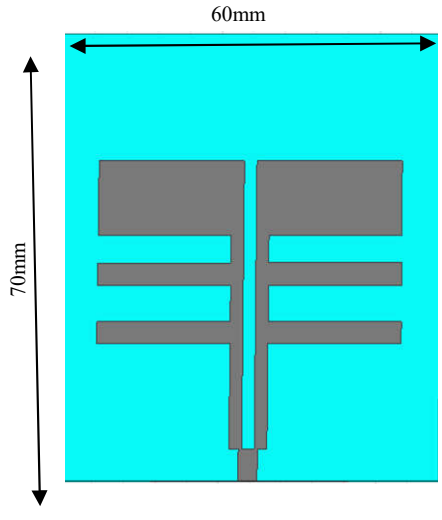

Fig a Top view of the patch Stage 2

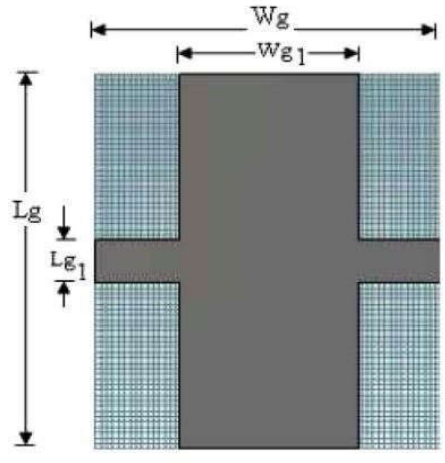

Fig b) bottom view of the metasurface antenna

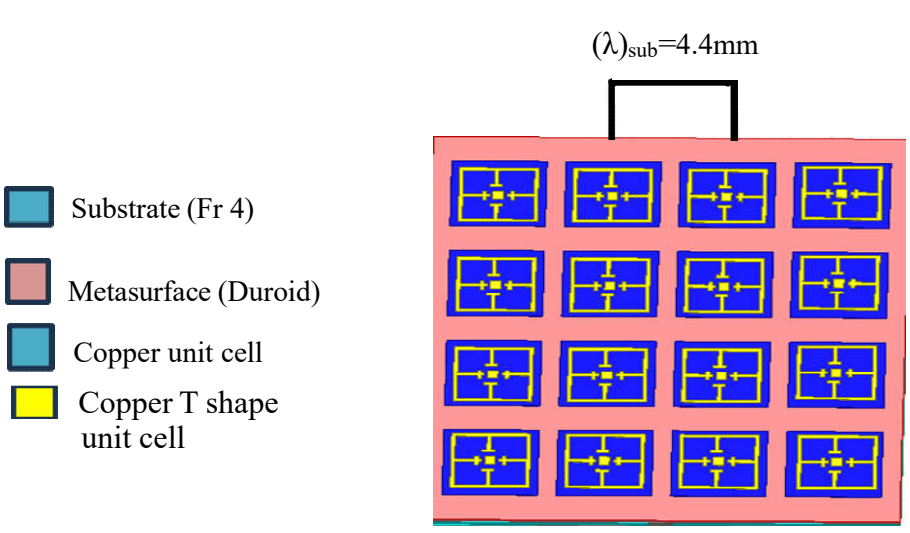

Fig c. Top view of stage3

As we get closer to the fifth-generation (5G) revolution, the requirement for efficient and adaptable antenna systems to support these advancements is greater than ever [5]. The 3-6 GHz frequency range is very important for the rollout of 5G mobile broadband since it strikes a balance between capacity, data rates, and coverage.

of the split rings, sub-wavelength resonance of the patch antenna can be achieved with a good impedance match and radiation characteristics [20].

TABLE-1. Optimized dimensions of Metasurface antenna.

Parameters	Values (in mm)	Parameters	Values (in mm)
Ls	70	W1	23
Ws	60	W2	3
H	1.6	g	2
L1	11.7	d	2
L2	33.5	Lg1	3
L3	5	Wg1	31

In Fig. 1 Key characteristics are carefully considered in the finely created antenna design shown in Fig. 1. A suitable platform for the antenna structure is provided by the substrate height, which is chosen at 2.2mm. In order to attain compactness and preserve structural integrity, a thin patch height of 0.035mm is selected [5]. The impedance matching and radiation characteristics of the antenna are optimised by the thoughtful placement of the slots.

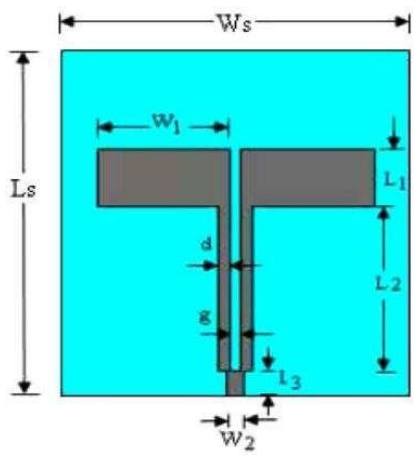

a) Top view of stage 1

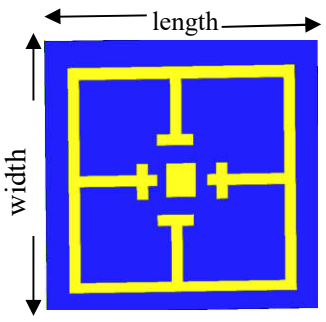

b) Single unitcell

Parameters	Dimensions(mm)
Length	12
Width	12
Thickness	0.05
Substate	Copper

A patch with T-shaped and rectangular slots (1 mm radius) and a 4x4 metasurface grid are combined to create the Metasurface antenna concept [6]. This design uses the metasurface in conjunction with a FR -4 substrate (relative permittivity = 1.2 and loss tangent = 0.02) that has a slotted patch.[8] The dimensions of the MS and the Rectangular are the same (0.6λ0×λ0×0.09λ0 mm3, where λ0 is the free space wavelength at 7.1 GHz) [3]. Ansys HFSS software has been used for all improvements and assessments of the suggested antenna [7].

The Microstrip patch antenna has a 400 MHz bandwidth at the first band and a 900 MHz bandwidth at the second band when it first works, with a return loss of 36 dB [3]. A 4×4 MS was then integrated, resulting in an enhanced S11 of -38 dB and a wider bandwidth of 3.29 GHz (5.17 GHz-7,1 GHz).

II. RESULTS

TABLE-2: Comparison of each evolution of Metasurface antenna.

Configuration	Resonance frequency and band (GHz)	Reflection coefficient (dB)	Impedance Bandwidth (MHz)	Gain (dB)
Stage 1	3.40	-18.37	114	2.54
	5.00	-22.88	211	3.35
	5.83	-24.85	217	6.65
Stage 2	3.7	-21.46	109	4.04
	4.5	-14.5	96	4.5
Stage 3	4.1	-25.88	145	5.01
	5.9	-22.15	600	5.52
Proposed antenna	5.1	-38.35	800	7.95
	5.4	-36.76	780	5.85
	6.9	-26.44	920	8.24

HFSS microwave studio was used to simulate the suggested antenna model [13]. Fig. 2 displays the antenna's simulated outcome with regard to return loss. Three resonant bands—5.1 Hz, 5.4 GHz, and 6.9 GHz—are displayed in the simulated results [6]. At two working frequencies, a return loss of -38.76dB, -36.76dB, and -26.44dB is noted [20].

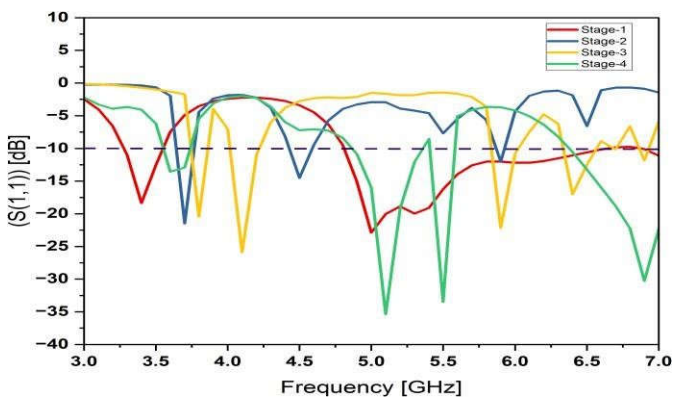

Fig.2 The Reflection coefficient response of slots on Metasurface antenna.

The evolution of the Metasurface antenna was depicted in Fig. 2. The basic antenna is shown in Yellow, followed by the one-slot antenna in Blue when a rectangular slot was added, the rectangular slot antenna in Red at stage 3, and finally the antenna in Green when a Metasurface was added [15].

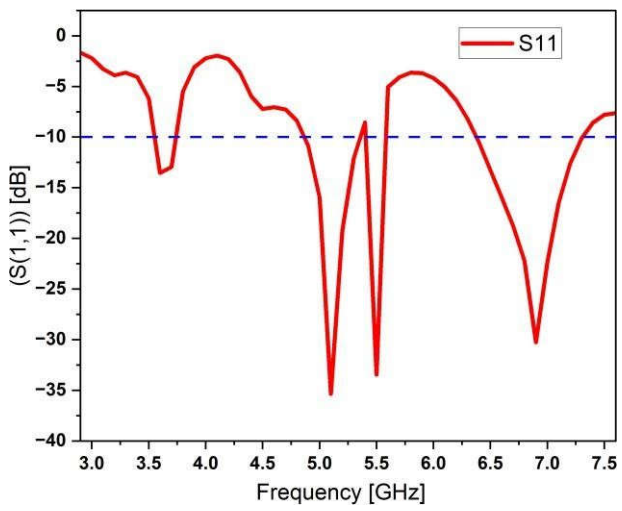

Fig.3 The Metasurface antenna return loss (S_{11}(dB)).

The gain plot of the Metasurface patch antenna is shown Fig. 4. The resonating frequency 2.45GHz with 3.67dB, 5.13GHz with 9.18dB and 5.46GHz with 8.24dB is observed [2].

The gain 3d polar plot of the metasurface patch antenna is shown below [6]:

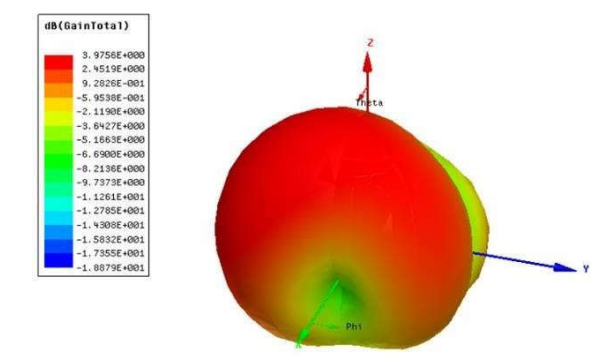

(a)

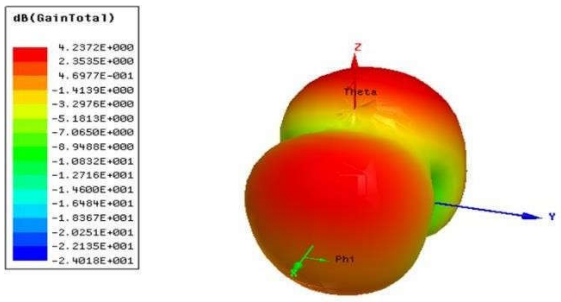

(b)

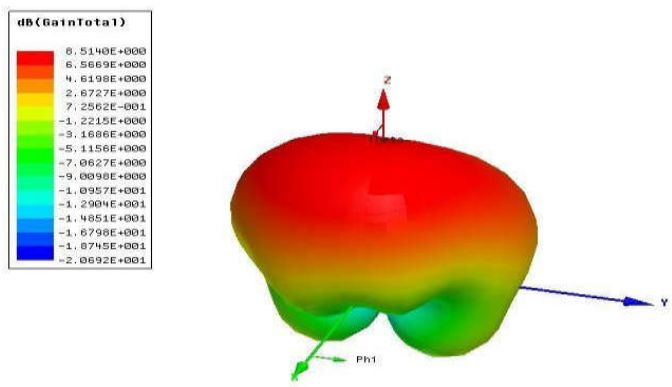

(c)

Fig. 4 The metasurface antenna gain at (a) 3.45GHz, (b) 5.1GHz c)5.4GHz .

Figure 5 displays the far field radiation maps for the patch's E and H-planes. The H-field radiation pattern is less than the E-field, according to the observation [6].

Fig. 5 shows the normalized far-field radiation characteristics linear polarization (Co-polar) and linear-polarization (X-polar) of both E(YZ)-plane, H (XZ)-planes at 5.1 GHz, 5.4 GHz, 6.9 GHz frequency is presented [14].

The far field radiation plots for E and H-planes of the patch is shown Fig 5. From the observation the H-field radiation pattern is less than E-field [17].

Fig. 5 shows the normalized far-field radiation characteristics linear polarization (Co-polar) and cross-polarization (X-polar) of both E(YZ)- plane, H (XZ)-planes at 5.45 GHz, 5.1GHz,
3.45 GHz frequency is presented [2].

The proposed antenna has been compared with previously reported metasurface type antenna structures as listed in Table I [2]. It has been seen that the presented antenna achieves bandwidth enhancement over the operating band in comparison to the reported ones maintaining similar amount of gain [2].

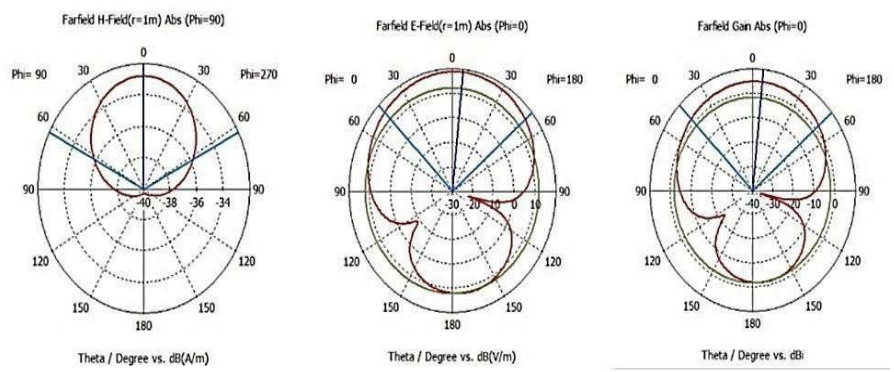

(a) (b) (c)

Fig 5 .H field Radiation patterns of the proposed antenna

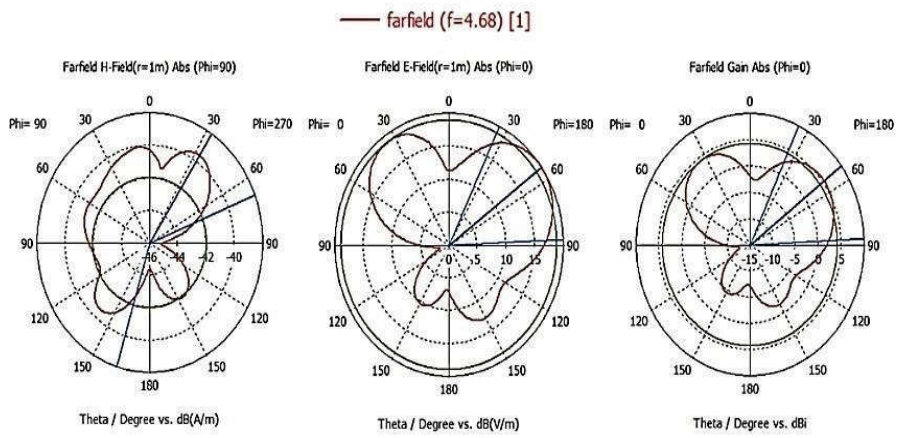

Fig 5. E field Radiation patterns of the proposed antenna

Fig. 5 shows the current distributions of Metasurface antenna at each resonant frequency [8]. In Fig.5 the maximum current concentrates at 3, 4, 5 slits with 190.5 *Alm* which leads to the resonance of 5.45 GHz frequency, for the second resonant frequency the current distribution is nearly same as that of first frequency (2.8 Alm) and for the third resonant frequency the proposed antenna the current distribution is maximum at 200.5 *Alm [1]*.

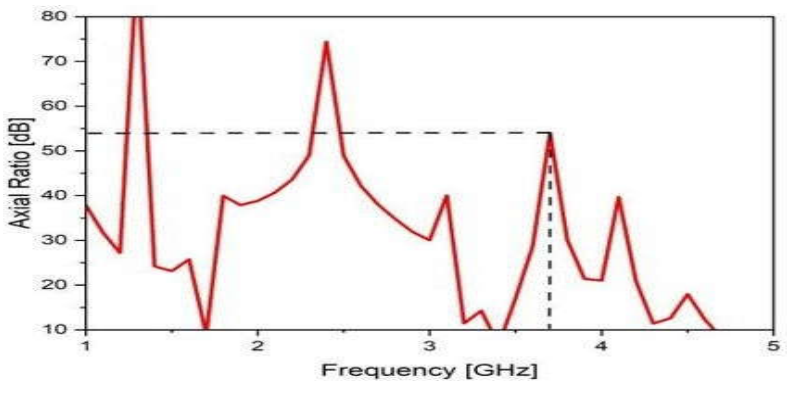

Fig.6 The Metasurface antenna Axial ratio

The axial ratio is a measure of the polarization purity of the electromagnetic radiation emitted by the antenna. It indicates the degree to which the antenna radiates or receives a particular polarization state compared to another orthogonal state.

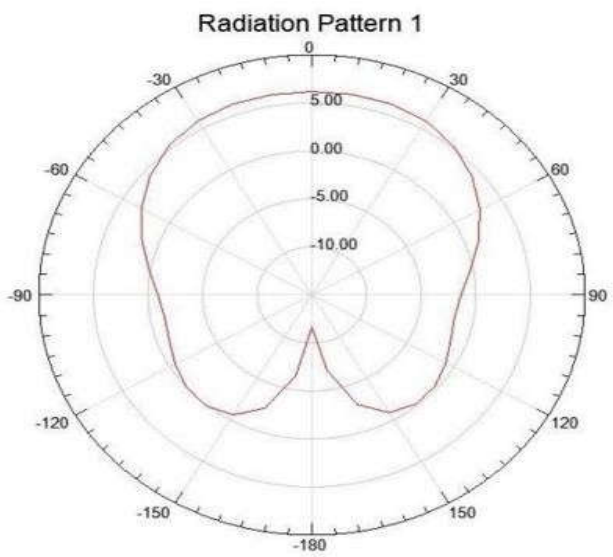

Fig.7 The Metasurface antenna Radiation Pattern

The radiation patterns of the antenna in both the planes have been investigated as depicted in Fig. 5. It is observed that theantenna offers boresight radiation in both the planes at 7.1 GHz. Further, the cross-polarized components are significantly down compared to the co-polarized ones.

CURRENT DISTRIBUTIONS:

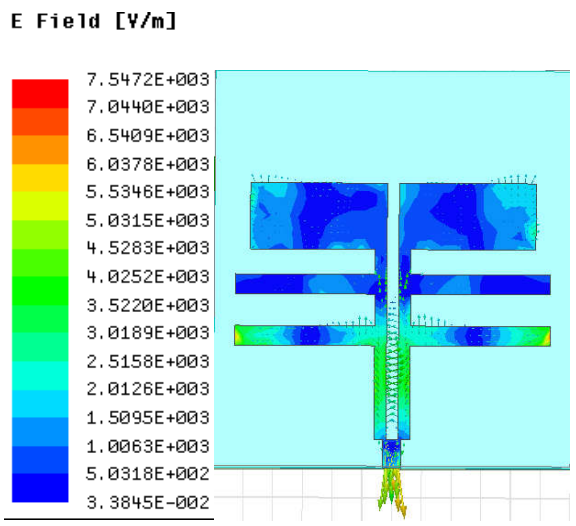

Fig. 8. Surface current distributions in the patch at 5.1GHz

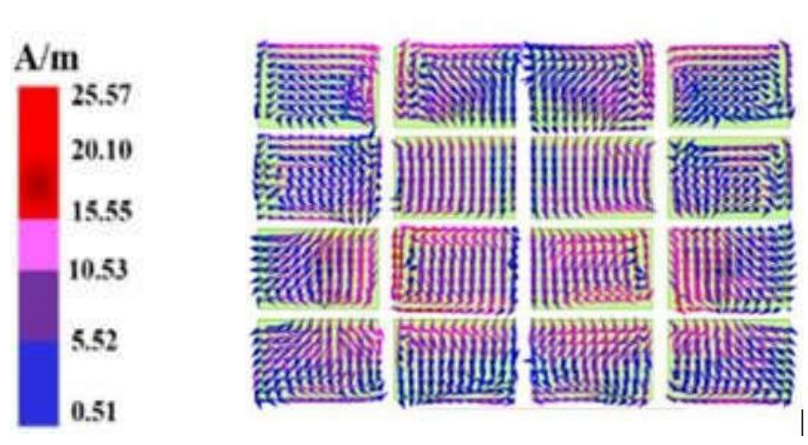

Fig 9. Surface current distributions in the Metasurface at 5.1GHz

The surface current distributions have been studied at both the surfaces of the antenna at 5.1 GHz. It is observed that thesurface currents are intense at the patch as well as the slot positions as see from Fig. 4. The surface currents have also been enhanced at the center of the MS layer as illustrated in Fig. 4.

The current distributions of the Metasurface antenna at each resonant frequency are displayed in Fig. 5. The resonance of 5.45 GHz frequency is caused by the maximum current concentration in Fig. 10(a) at 1, 2, and 3 slits with 25.57 A/m. For the second resonant frequency, the current distribution is almost the same as that of the first frequency (20 A/m), and for the third resonant frequency of the proposed antenna, the current distribution is maximum at 25.57 A/m

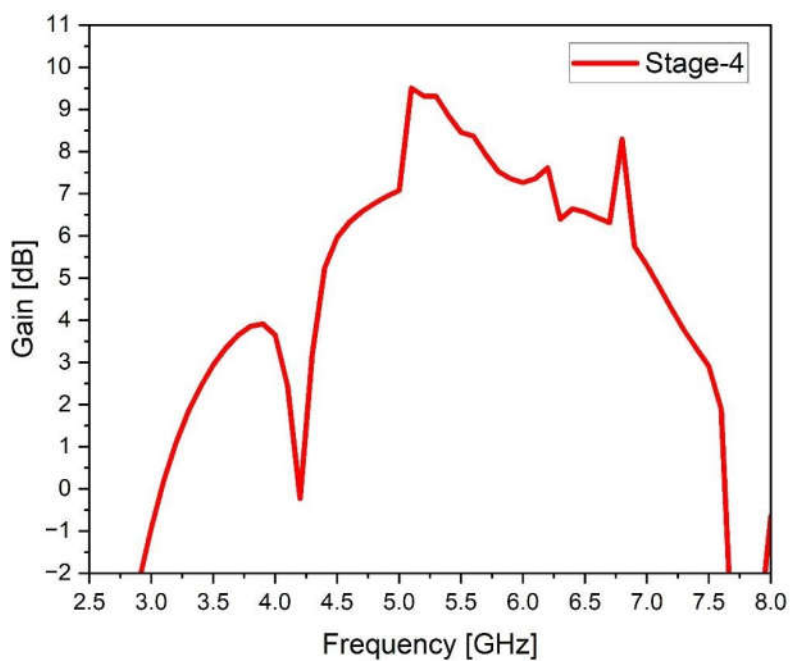

Fig 10 The gain graph of the proposed antenna

The graph showing Gain of dual band microstrip patch antenna and maximum peak is observed at 5.1 GHz with 9.15dB [2].

The antenna's overall performance is shown by the gain graph at 5.1 GHz with a 9 dB gain, which is helpful for designing and optimising wireless communication systems that use this frequency range [3].

Plotting frequency on the x-axis and gain on the y-axis is the resultant gain graph [5]. This graph is examined by engineers in order to determine the antenna's resonance frequencies, which are where it achieves its maximum gain, and to evaluate its bandwidth, which shows the range of frequencies across which reasonable performance is maintained [15]. Through close examination of the gain graph, engineers can tailor antenna designs to particular application needs, guaranteeing that the specifications are met [6]. The gain graph also helps validate antenna designs by enabling engineers to compare goal gain expectations with simulated performance [9]. Essentially, engineers may fine-tune antenna designs for best performance in a variety of wireless communication and radar applications with the help of the gain graph in HFSS [10].

TABLE-3: Comparison of existing antenna models to the proposed Metasurface antenna.

Ref. No	Operating frequency (GHz)	Reflection coefficient (dB)	Substrate material (εr, δ)	Gain (dBi)	Band width (GHz)	Antenna size (dimensions, mm^3)
1	2.4	−27.1	Fr-4 (4.4, 0.02)	2.53	0.43	90 × 36 × 0.8
	9.5	−16.2		2.82	0.83	
2	2.43	−14.5	Fr-4 (4.4, 0.02)	2.14	0.24	55 × 24 × 1.6
	5.2	−24.2		3.59	3.01	
3	5.4	−34.3	Fr-4 (4.4, 0.02)	2.4-2.8	0.7	25 × 40 × 1.6
	5.5	−15.1		1.9-2.1	0.5	
	5.2	−19.8		2.9-3.5	0.6	
	5.8	−13.58		2.6-3.2	0.19	
	6.8	−32.1			7	
Metasurface antenna	5.15	-38.3	Fr-4 (4,4,0.02)	7.95	0.106	70x 60x1.6
	5.4	-36.4		5.56	0.105	
	6.9	-26.27		8.24	0.24	

TABLE-3: Comparison of existing antenna models to the proposed Metasurface antenna

The proposed antenna has been compared with previously reported metasurface type antenna structures as listed in Table -3 [2]. It has been seen that the presented antenna achieves bandwidth enhancement over the operating band in comparison to the reported ones maintaining similar amount of gain [2].

III. CONCLUSION

This work presents the dual band metasurface patch antenna. The frequency at which resonance is recorded are 5.1GHz, 5.5GHz, and 6.9GHz, with corresponding return losses of -38.3dB, -33.22dB, and -26.96dB. There is less than two VSWR. The suggested antenna is functional for C-band uses. The measured data and the simulation agree quite well. This antenna is suited for mobile and flexible wireless applications due to its conformability, compactness, and flexibility**.**

IV. REFERENCES

[1]. *Jin Zhang, Shuai Zhang and Gert Frølund Pedersen: "Dual-Band Structure Reused Antenna Based on Quasi-Elliptic Bandpass Frequency Selective Surface for 5G Application" IEEE Transactions on Antenna and Propagation, vol. 68, No. 11, November 2020.*

[2]. Vannithamby and S. Talwar, Towards 5G: Applications, Requirements and Candidate Technologies. Hoboken, NJ, USA: Wiley, 2017.

[3]. J A. Sheersha, N. Nasimuddin, and A. Alphones, ''A high gain wideband circularly polarized antenna with asymmetric metasurface,'' Int. J. RF Microw. Comput. -Aided Eng., vol. 29, no. 7, Jul. 2019, Art. no. e21740

[4] H. Attia, M. L. Abdelghani, and T. A. Denidni, ''Wideband and high-gain millimeter-wave antenna based on FSS Fabry–Perot cavity,'' IEEE Trans. Antennas Propag., vol. 65, no. 10, pp. 5589–5594, Oct. 2017.

[5] N. Hussain, H. H. Tran and T. T. Le, "Single-layer wideband high-gain circularly polarized patch antenna with parasitic elements," AEU-International Journal of Electronics and Communications, vol. 113, pp. 152992, 2020.

[6] C. E. Santosa and J. T. Sri Sumantyo, "Gain enhancement of C band linearly-polarized microstrip antenna with square parasitic patch for airborne LP-SAR sensor," in Progress in Electromagnetics Research Symposium, Toyama, Japan, pp. 858–863, 2018.

[7] A. Iqbal, A. Smida, A. J. Alazemi, M. I. Waly, N. K. Mallat et al., "Wideband circularly polarized MIMO antenna for high data wearable biotelemetric devices," IEEE Access, vol. 8, no. 2020, pp. 17935–17944, 2020.

[8] W. E. I. Liu, Z. N. Chen, and X. Qing, ''Broadband low-profile L-Probe fed metasurface antenna with TM leaky wave and TE surface wave resonances,'' IEEE Trans. Antennas Propag., vol. 68, no. 3, pp. 1348–1355, Mar. 2020.

[9] S. Ladan, A. B. Guntupalli, and K. Wu, "A high-efficiency 24 GHz rectenna development towards millimeter-wave energy harvesting and wireless power transmission," IEEE Trans. Circuits Syst. I., Reg. Papers, vol. 61, no. 12, pp. 3358–3366, Dec. 2019

[10] R. Lu, C. Yu, Y. Zhu and W. Hong, "Compact millimeter-wave end fire dual-polarized antenna array for low-cost multibeam applications", IEEE Antennas Wireless

Propag. Lett., vol. 19, no. 12, pp. 2526-2530, Dec. 2020.

[11] Y. Zhu and C. Deng, "Millimeter-wave dual-polarized multibeam end fire antenna array with a small ground clearance", IEEE Trans. Antennas Propag., vol. 70, no. 1, pp. 756-761, Jan. 2022.

[12]. Yang and S. Zhang, "Dual polarized wide-angle scanning phased array antenna for 5G communication system" in IEEE Trans. Antennas Propag., Jan. 2022.

[13] P. K. Panda and D. Ghosh, ''Isolation and gain enhancement of patch antennas using EMNZ superstrate,'' AEU Int. J. Electron. Commun., vol. 86, pp. 164–170, Mar. 2018.

[14] A. K. Rashid, Z. Shen, and B. Li, "An elliptical bandpass frequency selective structure based on microstrip lines," IEEE Trans. Antennas Propag., vol. 60, no. 10, pp. 4661–4669, Oct. 2012.

[15] C. Mao, S. Gao, Y. Wang, Q. Chu, and X. Yang, "Dual-Band Circularly Polarized Shared-Aperture Array for C-/ X-Band Satellite Communications," IEEE Trans. Antennas Propag., vol. 65, no. 10, pp. 5171–5178, Oct. 2017.

[16]. S. Zhu, H. Liu, Z. Chen, and P. Wen, ''A compact gain-enhanced Vivaldi antenna array with suppressed mutual coupling for 5G mm Wave application,'' IEEE Antennas Wireless Propag. Lett., vol. 17, no. 5, pp. 776–779, Mar. 2018.

[17] W. E. I. Liu, Z. N. Chen, and X. Qing, "Miniature wideband nonuniform metasurface antenna using equivalent circuit model," IEEE Trans. Antennas Propag., vol. 68, no. 7, pp. 5652–5657, Jul. 2020.

[18]. S. Zhu, H. Liu, Z. Chen, and P. Wen, ''A compact gain-enhanced Vivaldi antenna array with suppressed mutual coupling for 5G mm Wave application,'' IEEE Antennas Wireless Propag. Lett., vol. 17, no. 5, pp. 776–779, Mar. 2018

[19] P. K. T. Rajanna, K. Rudramuni, and K. Kandasamy, ''A wideband circularly polarized slot antenna backed by a frequency selective surface,'' J. Electromagn. Eng. Sci., vol. 19, no. 3, pp. 166–171, Jul. 2019

[20] R. A. Iqbal, O. Saraereh, A. Bouazizi, and A. Basir, ''Metamaterial-based highly isolated MIMO antenna for portable wireless applications,'' Electronics, vol. 7, no. 10, p. 267, 2018.

[21]. S. Zhu, H. Liu, Z. Chen, and P. Wen, ''A compact gain-enhanced Vivaldi antenna array with suppressed mutual coupling for 5G mm Wave application,'' IEEE Antennas Wireless Propag. Lett., vol. 17, no. 5, pp. 776–779, Mar. 2018.

[22] R. P. K. T. Rajanna, K. Rudramuni, and K. Kandasamy, ''A wideband circularly polarized slot antenna backed by a frequency selective surface,'' J. Electromagn. Eng. Sci., vol. 19, no. 3, pp. 166–171, Jul. 2019.

[23] W. E. I. Liu, Z. N. Chen, and X. Qing, "Miniature wideband nonuniform metasurface antenna using equivalent circuit model," IEEE Trans. Antennas Propag., vol. 68, no. 7, pp. 5652–5657, Jul. 2020.